

Short Communication

A Novel Synthetic Strategy for Pd₃Sn Nanoparticles Loaded Reduced Graphene Oxide as Electrocatalyst for the Ethanol-Tolerant Oxygen Reduction Reaction

Changyu Lu^{1,2,3}, Weisheng Guan^{1,*}, Tuan K. A. Hoang³, Yuliang Li¹, The Nam Long Doan³, Hongbin Zhao^{2,3,*}

¹ School of Environmental Science and Engineering, Chang'an University, 126 Yanta Road, Xi'an, 710054, PR China

² Department of Chemistry, College of Science, Shanghai University, 99 Shangda Road, Shanghai, 200444, PR China

³ Department of Chemical Engineering and Waterloo Institute for Nanotechnology, University of Waterloo, 200 University Avenue West, Waterloo, Ontario N2L3G1, Canada

*E-mail: pzpzlxl@163.com (Weisheng Guan); hongbinzhao@shu.edu.cn (Hongbin Zhao)

Received: 18 March 2015 / Accepted: 12 April 2015 / Published: 28 April 2015

A novel, two-step chemical reduction route is suggested to synthesize highly active and well-dispersed Pd₃Sn alloy nanoparticles supported on chemically reduced graphene oxide (rGO) for the alcohol-tolerant oxygen reduction reaction. In this work, molecular-level dispersions of individuals are easily obtained, and graphene oxide is served as the stabilization agent for Pd₃Sn nanoparticles, and as carbon support which is co-deposited with metal or alloy particles. Transmission electron microscopy, Raman and powder X-ray diffraction results show that Pd and Pd₃Sn nanoparticles are finely-dispersed on multi-layer rGO with well-controlled particle sizes, dispersities and composition uniformities. Electrochemical measurements confirm that Pd₃Sn/rGO exhibits higher oxygen reduction activity and alcohol-tolerant ability than the Pd/rGO thanks to the smaller sizes of Pd₃Sn nanoparticles and the strong interaction between metal and rGO. This new strategy provides a facile route to synthesize multicomponent alloy loaded rGO composites for use in electro-catalysis.

Keywords: Methanol Electrocatalytic Oxidation, Pd₃Sn Nanoparticles, Reduced Graphene Oxide, Oxygen Reduction Activity, Alcohol-tolerant Ability

1. INTRODUCTION

Oxygen reduction reaction (ORR)—one of the most important reactions in chemistry that involved complicated redox processes [1]—has been studied for several decades because of its wide

applications, especially in energy conversion, alternative resource utilization and environmental protection. Till now, Pt-based catalysts are considered as the most promising oxygen reduction catalyst thanks to their high catalytic activity, and the carbon supported Pt-based nanoparticles are the most widely good compromise between electronic conductivity and surface area [2, 3]. Unfortunately, high cost and low ORR activity of the noble metal Pt forces us to search for alternative materials, among them are including Pt-based alloys, Pd-based alloys and other transition metal oxide composites. Pd-based alloys catalysts [4-8], including PdFe, PdSn and PdCo alloys, have been studied as oxygen reduction catalysts because of their low cost. Nevertheless, low electrochemical activity still limits the application of the aforementioned alloys. Therefore, research efforts have been made to enhance electrochemical activity and catalyst utilization by employing high specific surface carbon supports and small alloy particle sizes, which shows promising potential.

Reduced graphene oxide (rGO) sheets—one-atom-thick two-dimensional layers of sp^2 -bonded carbon—are predicted to have a range of unusual properties, such as remarkably in-plane value, fracture strength, similar defects with carbon nanotubes (CNTs), high specific surface area, high conductivity and electrochemical stability [9-11]. Since its first discovery, rGO has attracted great attentions and the catalysts supported on rGO have higher catalytic activities than those supported on traditional carbon materials (CNTs, XC72, active carbon) [9, 12-14]. Unfortunately, pure rGO is difficult to dissolve in water because of its hydrophobic surface, which limits its direct application as catalyst support. Compared with rGO, graphene oxide (GO) is readily soluble in both protic and aprotic solvents, such as water, dimethyl formamide (DMF) and N-methyl-2-pyrrolidone (NMP). Thus it should be an ideal method to synthesize different metals supported rGO from GO by using chemical reduction route. It is worth noting that the numerous oxygen functional groups on the surface of GO, such as $-COOH$, $-OH$ and $C=O$, render it to be too electrically insulating to use as a catalyst support; however, chemical reduction using hydrazine hydrate and ethanediamine can restore the conductivity by several orders of magnitude [15, 16] by removal of oxygen and recovery of aromatic double-bonded carbons. Even after a long reaction period using hydrazine hydrate as reducing agent, this process does not completely repair GO to pure rGO and thus, some oxygen containing groups still remain on reduced rGO surface. Thus, this rGO is still conductive and possesses chemically active defect sites making it a promising candidate for use as the carbon support in catalysis. However, the important problem which must be solved when using rGO as catalyst support is that metal/rGO composites synthesized by one-pot co-reduction method using mixtures of GO and metal ions usually causes separation of rGO from metal particles. Therefore, it is difficult to obtain well-dispersed metal-rGO composite by using single reducing agent. Besides, in most literatures, alloy catalysts were usually synthesized by changing the pH of reaction system and selecting weak reducing agents [4-7]. Up to date, only a few reducing agents can be used to reduce GO, noble metals and transition metals at the same time in synthesizing alloy catalysts with rGO as support. Although hydrazine hydrate is one of the best reducing agent of GO, it can not reduce noble metals and transition metals at comparable reaction rates, thus leads to low alloying degrees. In this case, mixed reducing agents and synthesis route are expected to obtain alloy-rGO catalysts.

Hence, we suggest here a new approach for the preparation of graphene-metal composites via complete exfoliation of graphite and molecular-level dispersion of individuals, followed by a two-step

chemical reduction of Pd and Sn containing precursors and GO using ethylene glycol-NaOH (EG-NaOH) and hydrazine hydrate as reducing agent. Using this method, fine-alloying Pd₃Sn nanoparticles loaded rGO composite was obtained successfully. GO not only served as the stable scaffold for the deposition of metal particles, but also as the support for Pd₃Sn nanoparticles after it was reduced to rGO. Cyclic voltammetry (CV) and Linear sweep voltammetry (LSV) were used to investigate electrochemical activity and oxygen reduction performance of Pd and Pd₃Sn loaded rGO composites.

2. EXPERIMENTAL

2.1. Fabrication of Pd₃Sn/rGO composites

GO was synthesized from natural flake graphite powder by a modified Hummers method [9]. In a typical synthesis, 2.0 g of graphite powder was put into cold (<4 °C) concentrated H₂SO₄ solution (46 mL). Then, 1.0 g of NaNO₃ and 6.0 g of KMnO₄ was added gradually under stirring, and the temperature of the mixture was kept at below 10 °C in ice-water bath for 2 hours. Subsequently, the mixture was stirred at 35 °C during 30 minutes. Then, 92 mL of warm double deionized (DDI) water was added dropwise and the temperature was kept constantly at 98 °C for 15 minutes. After that, the obtained suspension was further diluted to approximately 140 mL with DI water. Then, 20 mL of fresh H₂O₂ (5%) was added to the mixture to reduce the residual KMnO₄. The obtained mixture was isolated by centrifugation and washed with 5 wt% HCl for several times until SO₄²⁻ was not detected by BaCl₂ solution. Finally, the residual was dried at 40 °C for 24 hours.

The sequential synthetic process for the Pd/rGO and the Pd₃Sn/rGO consists of two steps: (1) 50 mg dried GO was re-dispersed in DDI water by ultrasonication. 2 mL EG, PdCl₂ (20 mg Pd) and/or SnCl₂·4H₂O (17 mg) solution were introduced into the GO-water solution under vigorously stirring for one hour. 1 M NaOH-EG solution was added dropwise to modify pH to 12. The suspension was heated up 110 °C and kept condensation for 10 hours. (2) 5 mL 85% hydrazine hydrate in 20 mL DDI water was slowly added into the suspension and keep condensation for 24 hours to allow the nucleation and growth of the metals or alloys, and GO-stabled Pd₃Sn and Pd nanoparticles suspension were obtained. Next, the obtained suspensions were cooled to room temperature and the solid products were isolated via centrifugation; these products were washed with DDI water and ethanol for three times; dried at 40 °C in a vacuum oven for 12 hours. The obtained composites were named Pd₃Sn/rGO and Pd/rGO, respectively.

2.2. Structural analysis

The structures of the products were characterized by a PANalytical (X' Pert PRO) diffractometer using Cu K α radiation ($\lambda = 0.1541$ nm) in a scan range of 10–90°. The morphologies were characterized by transmission electron microscope (TEM, JEOL JEM-2100F, 200 kV). A Uv-Vis Raman microscope (Uv-Vis Raman System 1000, Renishaw, UK) was used to investigate the reduction degree of rGO with wavenumber range from 1200 cm⁻¹ to 1800 cm⁻¹. A prodigy inductively-coupled

plasma atomic emission spectrometer (ICP-AES) was used to quantify the contents of Pd and Sn metals in the synthesized catalysts after digesting the Pd/rGO and Pd₃Sn/rGO composites in HCl-HNO₃ system (1:3).

2.3. Electrochemical measurements

A potentiostat/galvanostat (Autolab PGSTAT30, Holland) was used for the CV and CA measurements when samples were placed in a single compartment glass cell. A clean glassy carbon (GC) electrode (0.071 cm² geometric area) was used as working electrode, a saturated calomel electrode (SCE) and a platinum foil (1cm²) as reference and counter electrodes, respectively. The experiments were carried out at room temperature in an aqueous solution containing 0.5 M H₂SO₄, 1 M alcohol concentration and the solution was saturated with high purity O₂ or N₂. The working electrode was prepared as following: the synthesized catalyst was dispersed ultrasonically in 1 mL Nafion-ethanol solution (Nafion wt% = 0.024) for 30 minutes to obtain a homogenous suspension. 10 μL of the suspension was coated onto the glassy carbon electrode, followed by drying in the air at room temperature. CV curves were recorded at a scan rate of 50mV/s by high pure N₂ saturation. LSV measurement was carried out under different scan rate (10, 20, 50, 100, 200 mV/s) by high pure O₂ saturation.

3. RESULTS AND DISCUSSION

3.1. Physico-chemical properties of Pd₃Sn/rGO and Pd/rGO

TEM micrographs and nanoparticle size distributions of the Pd/rGO and Pd₃Sn/rGO are displayed in Figure 1, which evidently reveal that the GO layers is dominantly multi-sheet structure (Figure. 1c) with several sheets and about 1 μm in length. TEM image of pure rGO obtained when using hydrazine hydrate as reducing agent is shown in Figure.1d with several-layers sheet structure and slight crepes, which indirectly confirmed that hydrazine hydrate was an ideal reduced agent for GO reduction. It also can be seen from Figure 1a-b, similar dispersion of Pd and Pd₃Sn metal particles are well identified on the surface of rGO with slight agglomerations [17]. The agglomeration might be mainly ascribed to the long time reduction of GO at 120 °C which causes the crystalline growths of metal and alloy. The mean particle size of Pd and Pd₃Sn metal nanoparticles on Pd/rGO and Pd₃Sn/rGO is about 6.1 nm and 5.8 nm, respectively.

The Pd₃Sn nanoparticles is well-dispersed, thanks to the two-step chemical reduction method, which is visualized in Figure 2. In the first step, molecular-level dispersions of individuals (GO, Pd²⁺ and Sn⁴⁺) were obtained by ultrasonication, and Pd²⁺ and Sn⁴⁺ ions were adsorbed on the defects of GO thanks to the strong interaction between metal ions and GO. After EG-NaOH solution was dropped into the suspension, Pd²⁺ and Sn⁴⁺ ions were converted to associated hydroxides (Pd(OH)₂ and Sn(OH)₄) in GO-stabilised solution. Afterwards, these two hydroxides were reduced to Pd₃Sn alloy by EG in alkaline condition. GO was employed as a stabilizing agent for metal nanoparticles in this step.

Then GO was reduced to rGO by adding hydrazine hydrate as reducing agent. Hydrazine hydrate also reduces metal hydroxides to metal or alloy nanoparticles, which were instantly adsorbed on the surface of rGO at the second reaction step. By the two-step chemical reduction method, the separation phenomenon of rGO from metal particles is successfully avoided. The special structure and abundant defects of rGO provide sites for metal particles to be adsorbed on its defects surface, which was formed in the incomplete reduction of GO [18]. This route is also adoptable for other multicomponent alloy catalysts loaded on rGO. ICP-AES results showed that Pd content in Pd/rGO and Pd₃Sn/rGO was 55.1% and 54.4%, respectively. The molar ratio of Pd to Sn in Pd₃Sn/rGO composite was 3.02.

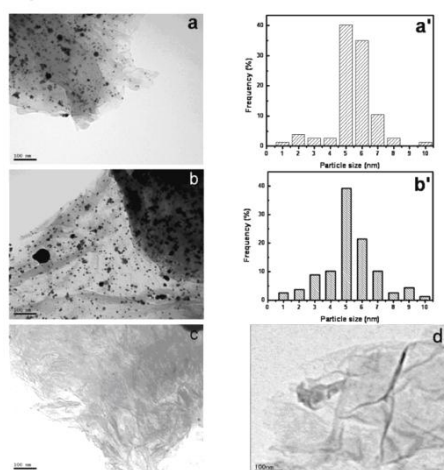


Figure 1. TEM images and the particle distribution of Pd/rGO (a, a'), Pd₃Sn/rGO (b, b'), GO (c) and rGO (d)

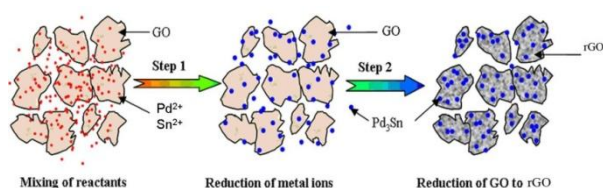


Figure 2. Scheme of two-step chemical reduction to synthesize Pd/rGO and Pd₃Sn/rGO catalysts

XRD patterns shown in Figure 3 confirm that obvious Pd (PDF#46-1043) and Pd₃Sn (PDF#37-0419) diffraction peaks are precisely indexed [19,20]. Besides, obvious diffraction peak (C-002) of RG at 24.8° are observed, while all the flake graphite diffraction peak at 27.5° and 55° and the GO diffraction peak (C-001) at 10.5° scarcely could be found in Pd/rGO and Pd₃Sn/rGO composites, which confirm successful reduction of GO by the hydrazine hydrate. The particle sizes of Pd and Pd₃Sn calculated by Scherrer equation are 5.2 nm and 5.7 nm, respectively, slight larger than that of TEM statistics result. Otherwise, obvious Pd₃Sn diffraction peak is found around 52°, which further confirms the existence of Pd₃Sn alloy phase in the composite.

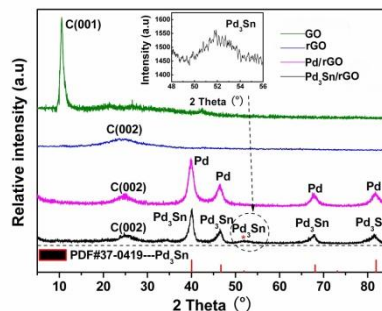


Figure 3. XRD patterns of GO, rGO, Pd/rGO and Pd₃Sn/rGO

Raman analysis (Figure 4) is used to investigate the reduction degree of GO. The I_G/I_D ratio of Pd/rGO and Pd₃Sn/rGO increased from 1.16 of GO to 1.26 and 1.27 of rGO, respectively, indicating sp^2 carbon increased and logically, an enhanced conductivity of rGO, which usually represents enhanced structural integrity [21]. It is worth noting that this ratio is far lower than the observed Raman result of flake graphite, indicating that the rGO obtained from flake graphite oxidation-ultrasonic exfoliation method still possesses some structural defects. These defects are identical to the surfaces of HNO₃ pretreated CNTs, which is beneficial for metal deposition. Optimistically, these incomplete structural defects provide more sites for metal adherence, thus the dispersion and utilization of Pd and Pd₃Sn are improved.

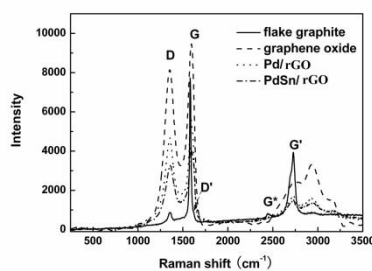


Figure 4. Raman spectrums of flake graphite, GO, Pd/rGO and Pd₃Sn/rGO

3.2. Electrochemical measurement

In the CV curves of Figure 5, the typical hydrogen adsorption/desorption peaks in the range of -0.3 V to 0.1 V on Pd₃Sn/rGO and Pd/rGO are obvious, which usually represents typical hydrogen adsorption/desorption on different Pd lattice planes. The electrochemical active specific surface of Pd₃Sn evaluated by the area of hydrogen adsorption/desorption peaks was higher than that of Pd/rGO. Higher electro-oxidation activity of Pd₃Sn/rGO should be attributed to high specific surface and defects of RG, which supply enough surface and absorption sites for Pd₃Sn adherence.

As discussed in literature, Pd₃Sn alloy is usually used as ethanol electro-oxidation catalysts

[22-23]. In our primary design, we wished to synthesize Pd₃Sn/rGO catalyst for ethanol electrochemical oxidation. Interestingly, a strange phenomenon was found in our study that the synthesized Pd₃Sn/rGO has almost no ethanol oxidation activity (Figure 5). Therefore, further research in different alcohol containing solutions was carried out to investigate whether there is a common rule of alcohol oxidation on the synthesized Pd₃Sn/rGO. CV curves show that all the small organic molecules, including methanol, ethanol, even HCHO, have no obvious oxidation peaks on Pd₃Sn/rGO modified GC electrode in N₂ saturation system. This result indicates significant alcohol-tolerant ability of Pd₃Sn/rGO catalyst. The reason for small organic molecules-tolerance on Pd₃Sn/rGO is still not understood. Here we suggest that there are at least two factors, including Sn metal in the Pd₃Sn alloy and rGO carbon support, which affects the adsorption and oxidation behaviors of small organic molecules on the synthesized Pd₃Sn/rGO composite. Sn metal in the Pd₃Sn alloy might modify the electronic orbitals of Pd, which increase the distance between Pd atoms and reduce the overlap between the electron cloud, and further changes the adsorption and oxidation behavior of small organic molecules and decrease the adsorption of intermediates of methanol oxidation. As for rGO, both side of rGO could provide adherence sites for Pd₃Sn nanoparticles, and Pd₃Sn nanoparticles were encapsulated into the interlamination of multi-layered rGO during the second step, thus a layer structured Pd₃Sn/rGO composite was obtained, which could change the adsorption behaviors of small organic molecules.

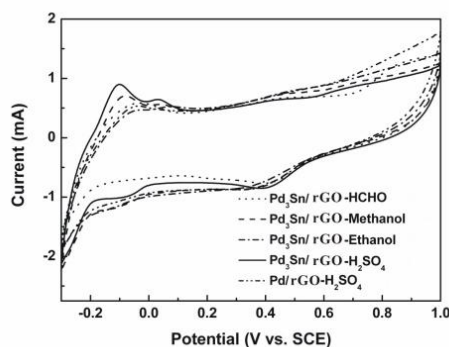


Figure 5. CV curves of Pd₃Sn/rGO catalyst in 1 M different alcohol + 1 M H₂SO₄ with scan rate of 50 mV/s by high pure N₂ saturation

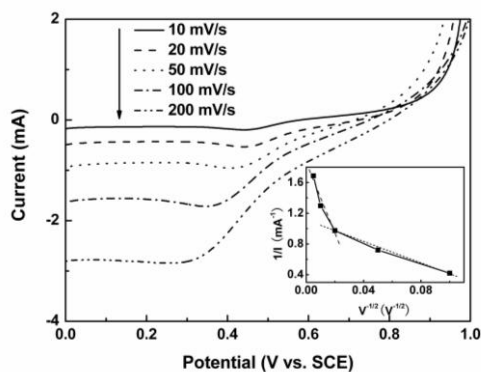


Figure 6. LSV curves of Pd₃Sn/rGO modified GC electrode in 1 M H₂SO₄ by high pure O₂ saturation. Illustration is the linear relationship between 1/I and 1/v^{1/2} around 0.4 V (vs. SCE).

On the contrary, the oxygen reduction peak current exists (around 0.4 V vs SCE) not only in H₂SO₄ but also in different organic molecules solution, shows no obvious change, which indicates stable- ORR-activity on Pd₃Sn/rGO composite and the existence of organic molecules does not affect the ORR performance on Pd₃Sn/rGO.

Further study of LSV with different scan rate (Figure 6) shows that ORR properties of synthesized Pd₃Sn/rGO catalyst exhibit an obvious ORR peak around 0.42 V (vs. SCE). The peak current density is consistent with the scan rate, which means that ORR on the Pd₃Sn/rGO is controlled by diffusion step under low scan rate. According to Randles-Sevick equation, there is a fine linear relationship between $1/I$ and $1/v^{1/2}$ around 0.4 V (vs. SCE). All our experiments confirm that Pd₃Sn/rGO catalyst shows promising application on oxygen reduction reaction with good alcohol-tolerance ability.

4. CONCLUSIONS

A two-step chemical reduction method with EG-NaOH and hydrazine hydrate as reducing agent is suggested to obtain well alloying Pd₃Sn loaded rGO composite. Well-dispersed Pd and Pd₃Sn nanoparticles deposited on rGO have been proved to possess homogenous size distribution around 5.5 nm. Pd₃Sn/rGO exhibits high alcohol-tolerance ability and excellent oxygen reduction activity, which is attributed to the higher specific surface of rGO as well as the strong interaction between metal nanoparticles and rGO. Tin modified Pd₃Sn alloy and multi-layered structure of rGO are two main reasons for the high alcohol-tolerance. The results presented in this paper indicate that the two-step chemical reduction method provides a facile route for synthesizing multicomponent alloy-RG composite for ORR and may be other electrochemical catalytic reactions.

ACKNOWLEDGEMENTS

The authors acknowledge the support from the China Scholarship Council (CSC NO.201406560003, 201406895017), Doctor Postgraduate Technical Project of Chang'an University (NO.2014G5290009), Fundamental Research Funds for the Central Universities (NO.2014G329207, 2014G2290017), Shanghai University International Cooperation and Exchange Fund, Shanghai Education Commission Innovation Project (14YZ016) and Shanghai University Discipline of Batteries Material Chemistry, Research and Development Project of Science and Technology of Shaanxi Province (No. 2013JQ2019), a Project funded by China Postdoctoral Science Foundation (No. 2014M552400) and National Training Projects of the University Students' Innovation and Entrepreneurship program (NO.201310710057, 201410710060).

References

1. R. Holze and W. Vielstich, *J. Electrochem. Soc.*, 131 (1984) 2298.
2. W.Y. Yuan, S.F. Lu, Y. Xiang and S.P. Jiang, *RSC Adv.*, 4 (2014) 46265.
3. Y.L. Zheng, P. Li, H.B. Li and S.H. Chen, *Int. J. Electrochem. Sci.*, 9 (2014) 7369.
4. J.Z. He, J.H. Zhao, Z. Run, S.S. Zheng and H. Pang, *Int. J. Electrochem. Sci.*, 9 (2014) 7351.
5. F.C. Zhu, M. Wang, Y.W. He, G.S. Ma, Z.H. Zhang and X.G. Wang, *Electrochim. Acta*, 148 (2014)

- 291.
6. S.G. da Silva, M.H.M.T. Assumpcao, J.C.M. Silva, R.F.B. De Souza, E.V. Spinace, A.O. Neto, and G.S. Buzzo, *Int. J. Electrochem. Sci.*, 9 (2014) 5416.
 7. M. Martin-Martinez, A. Álvarez-Montero, L.M. Gómez-Sainero, R.T. Baker, J. Palomar, S. Omar, S. Eser and J.J. Rodriguez, *Appl. Catal. B-Environ.*, 162 (2015) 532.
 8. F. Xiao, T. Fukuda, T. Kakeshita and K. Takahashi, *J. Alloy. Compd.*, 577 (2013) 323
 9. Y.H. Lu, M. Zhou, C. Zhang and Y.P. Feng, *J. Phys. Chem. C*, 113 (2009) 20156.
 10. S. Kellici, J. Acord, J. Ball, H.S. Reehal, D. Morgan and B. Saha, *RSC Adv.*, 4 (2014) 14858.
 11. J. Moreira, P. Angel, A.L. Ocampo, P.J. Sebastian, J.A. Montoya and Castellanos RH, *Int. J. Hydrogen. Energy*, 29 (2004) 915.
 12. X.C. Qiao, C.H. You, T. Shu, Z.Y. Fu, R.P. Zheng, X.Y. Zeng, X.H. Li and S.J. Liao, *Electrochem. Comm.*, 47 (2014) 49.
 13. M.K. Kumar, N.S. Jha, S. Mohan and S.K. Jha, *Int. J. Hydrogen. Energy*, 39 (2014) 12572.
 14. M. Chen, Y. Meng, J. Zhou and G.W. Diao, *J. Power. Sources*, 265 (2014) 11.
 15. S. Gilje, S. Han, M. Wang, K.L. Wang and R.B. Kaner, *Nano. Lett.*, 7 (2007) 3394.
 16. J.T. Robinson, F.K. Perkins, E.S. Snow, Z.Q. Wei and P.E. Sheehan, *Nano. Lett.*, 8 (2008) 3137.
 17. C.M. Sims, A.A. Ponce, K.J. Gaskell and B.W. Eichhorn, *Dalton. T.*, 44 (2015) 977.
 18. I.V. Lightcap, H.K. Thomas and V.K. Prashant, *Nano. Lett.*, 10 (2010) 577.
 19. P.T. Patil, A. Dimitrov, J. Radnik and E. Kemnitz, *J. Mater. Chem.*, 18 (2008) 1632.
 20. A. Devadas, S. Vasudevan and F. Epron, *J. Hazard. Mater.*, 185 (2011) 1412.
 21. K.N. Kudin, B. Ozbas, H.C. Schniepp, R.K. Prud'homme, I.A. Aksay and R. Car, *Nano. Lett.*, 8 (2008) 36.
 22. N. Li, Z.Y. Wang, K.K. Zhao, Z.J. Shi, S.K. Xu and Z.N. Gu, *J. Nnaosci. Nanotechno.*, 10 (2010) 6748.
 23. C. Bianchini and P.K. Shen, *Chem. Rev.*, 109 (2009) 4183.

© 2015 The Authors. Published by ESG (www.electrochemsci.org). This article is an open access article distributed under the terms and conditions of the Creative Commons Attribution license (<http://creativecommons.org/licenses/by/4.0/>).